Supplementary Materials

Function of triazenido compound for electrocatalytic hydrogen production catalyzed by platinum complex

Yun-Xiao Zhang, Chen-Neng Lin and Shu-Zhong Zhan*

Table of context

	$Pt(PPh_3)_2Cl_2$.
9	**Fig. S9.** CVs of 2.50 mM solution of HL with varying concentrations of acetic acid in DMF. Conditions: 0.10 M [n-Bu_4N]ClO_4 as supporting electrolyte, scan rate: 100 mV/s, glassy carbon working electrode (1 mm diameter), Pt counter electrode, Ag/$AgNO_3$ reference electrode. Ferrocene internal standard (*).
10	**Fig. S10.** Charge buildup versus time from electrolysis of blank (black), 9.32 μM HL (red), 9.32 μM $Pt(PPh_3)_2Cl_2$ (blue), the mixture of 9.32 μM HL and 9.32 μM $Pt(PPh_3)_2Cl_2$ (green), and 9.32 μM $Pt(PPh_3)_2$(L)Cl (violet) in DMF (0.10 M [n-Bu_4N]ClO_4) under -1.45 V versus Ag/$AgNO_3$.
11	**Fig. S11.** (a) CVs of complex $Pt(PPh_3)_2Cl_2$ in different concentration. (b) CVs of $Pt(PPh_3)_2Cl_2$ (0.25 μM) in different pH. Conditions: Glassy carbon working electrode (1 mm diameter), Pt wire counter electrode, Ag/AgCl reference electrode.
12	**Fig. S12.** (a) CVs of HL in different concentration. (b) CVs of HL (0.25 μM) in different pH. Conditions: 0.25 M phosphate buffered solution (pH 7.0), glassy carbon working electrode (1 mm diameter), Pt wire counter electrode, Ag/AgCl reference electrode.
13	**Fig. S13.** (a) GC traces after a 1-h controlled-potential electrolysis at −1.45V *vs* Ag/AgCl of 2.33 μM $Pt(PPh_3)_2$(L)Cl in 0.25 M phosphate buffer (pH 7.0). A standard of CH_4 was added for calibration purposes. (b) Measured (red) and calculated (black) pH changes assuming a 100% Faradic efficiency of complex during electrolysis. (the theoretical pH change over time can be calculated by the equation of $pH = 14 + \lg\frac{\sum It}{FV}$ where I = current (A), t = time (s), F = Faraday constant (96485 C/mol), V = solution volume (0.05 L).
14	**Fig. S14. (a)** GC traces after a 1-h controlled-potential electrolysis at −1.45 V *vs* Ag/AgCl of 2.33 μM $Pt(PPh_3)_2Cl_2$ in 0.25 M phosphate buffer (pH 7.0). A standard of CH_4 was added for calibration purposes. (b) Measured (red) and

	calculated (black) pH changes assuming a 100% Faradic efficiency of complex during electrolysis. (the theoretical pH change over time can be calculated by the equation of $pH = 14 + \lg\frac{\sum It}{FV}$ where I = current (A), t = time (s), F = Faraday constant (96485 C/mol), V = solution volume (0.05 L).
15	**Fig. S15.** (a) GC traces after a 1-h controlled-potential electrolysis at −1.45 V *vs* Ag/AgCl of 2.33 μM HL in 0.25 M phosphate buffer (pH 7.0). A standard of CH_4 was added for calibration purposes. (b) Measured (red) and calculated (black) pH changes assuming a 100% Faradic efficiency of complex during electrolysis. (the theoretical pH change over time can be calculated by the equation of $pH = 14 + \lg\frac{\sum It}{FV}$ where I = current (A), t = time (s), F = Faraday constant (96485 C/mol), V = solution volume (0.05 L).
16	**Fig. S16.** (a) Charge buildup versus time from 2.33 μM complex **1** in a 0.25 M buffer (pH 7.0) under -1.45 V *vs* Ag/AgCl. (b) Charge buildup versus time from 2.33 μM $Pt(PPh_3)_2Cl_2$ in a 0.25 M buffer (pH 7.0) under -1.45 V *vs* Ag/AgCl. (c) Charge buildup versus time from 2.33 μM HL in a 0.25 M buffer (pH 7.0) under -1.45 V *vs* Ag/AgCl.
17	**Eq. S1.** The calculation of TOF for $Pt(PPh_3)_2Cl_2$ (in DMF)
18	**Eq. S2.** The calculation of TOF for $Pt(PPh_3)_2(L)Cl$ (in DMF)
19	**Eq. S3.** The calculation of TOF for $Pt(PPh_3)_2(L)Cl$ (in buffer, pH 7.0)
20	**Eq. S4.** The calculation of TOF for ($Pt(PPh_3)_2Cl_2$ (in buffer, pH 7.0).
21	**Eq. S5.** The calculation of TOF for HL (in buffer, pH 7.0)

22	**Table S1.** Crystallographic data for **HL** and $Pt(PPh_3)_2(L)Cl$ **1**
23	**Table S2.** Selected bond lengths (**Å**) and angles (o) for **HL** and $Pt(PPh_3)_2(L)Cl$ **1**

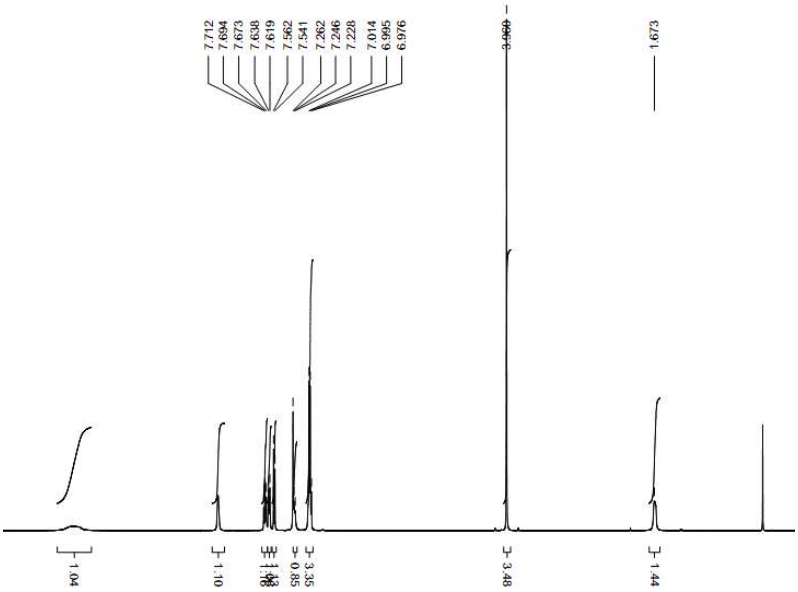

Fig. S1. ^1H NMR spectrum of ligand (HL)

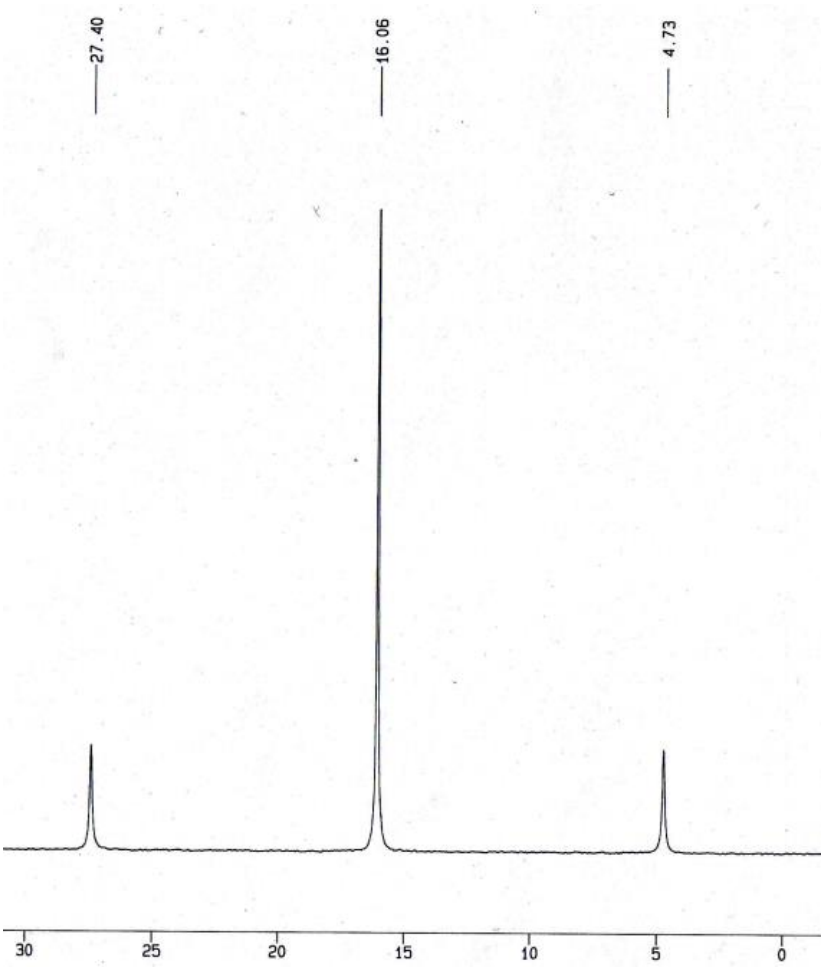

Fig. S2. ^{31}P NMR spectrum of $Pt(PPh_3)_2Cl_2$ in $CDCl_3$.

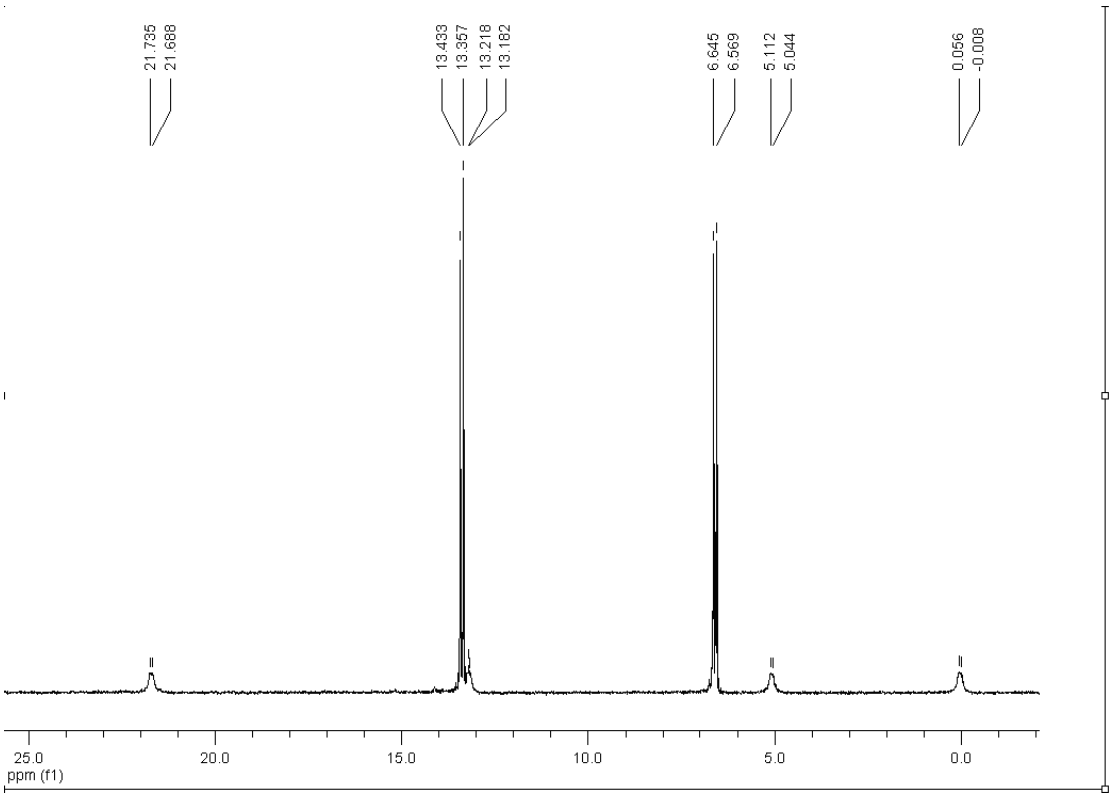

Fig. S3. ^{31}P NMR spectrum of complex **1** in $CDCl_3$.

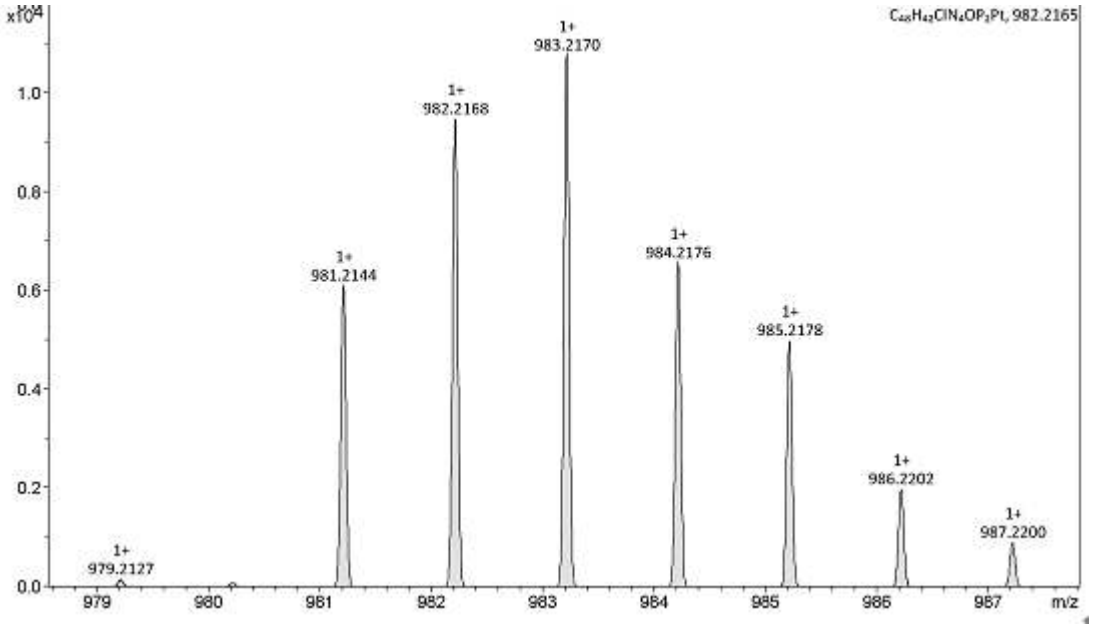

Fig. S4. ESI-MS of complex **1** in methanol.

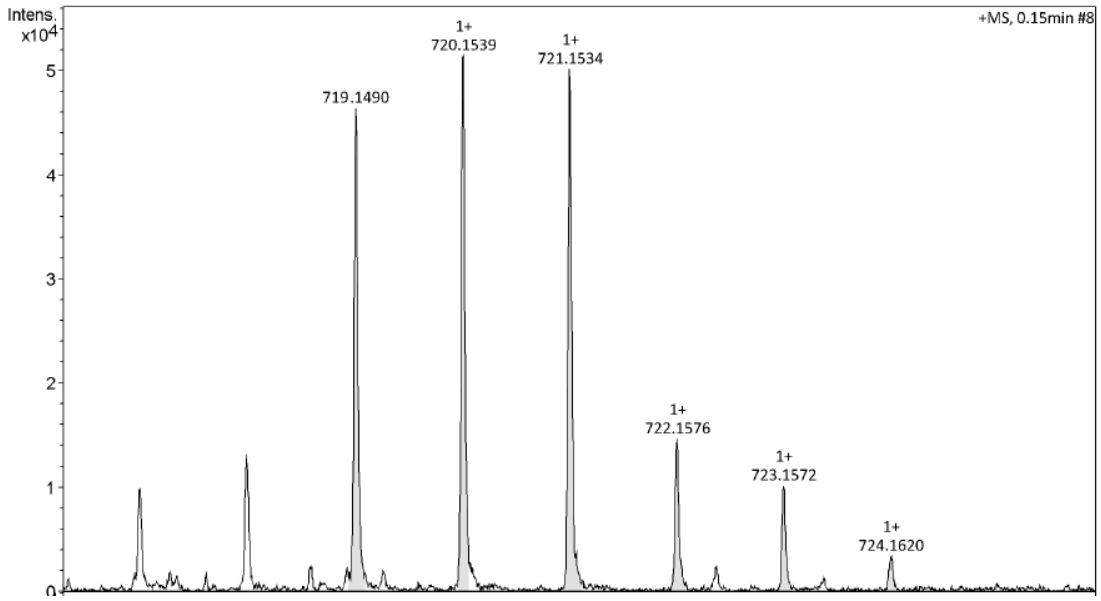

Fig. S5. ESI-MS of $Pt(PPh_3)_2Cl_2$ in methanol.

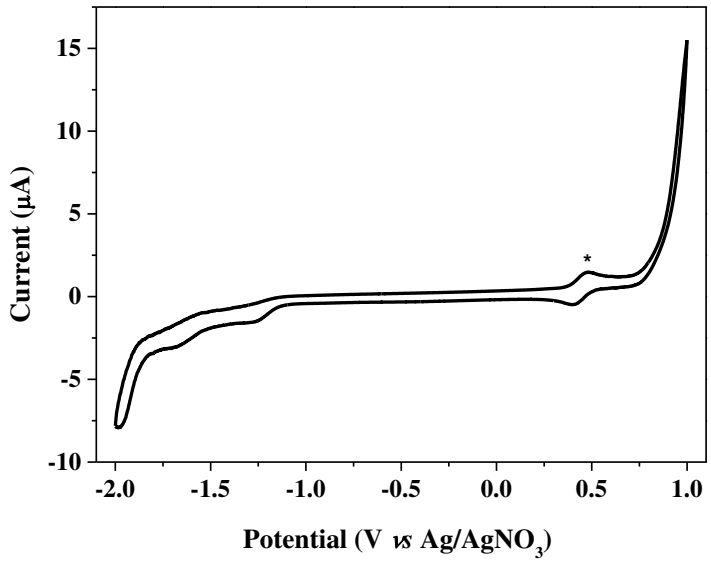

Fig. S6. CV of 2.50 mM HL in 0.10 M of [n-Bu_4N]ClO_4 DMF solution at a glassy carbon electrode and a scan rate of 100 mV/s, ferrocene internal standard (*).

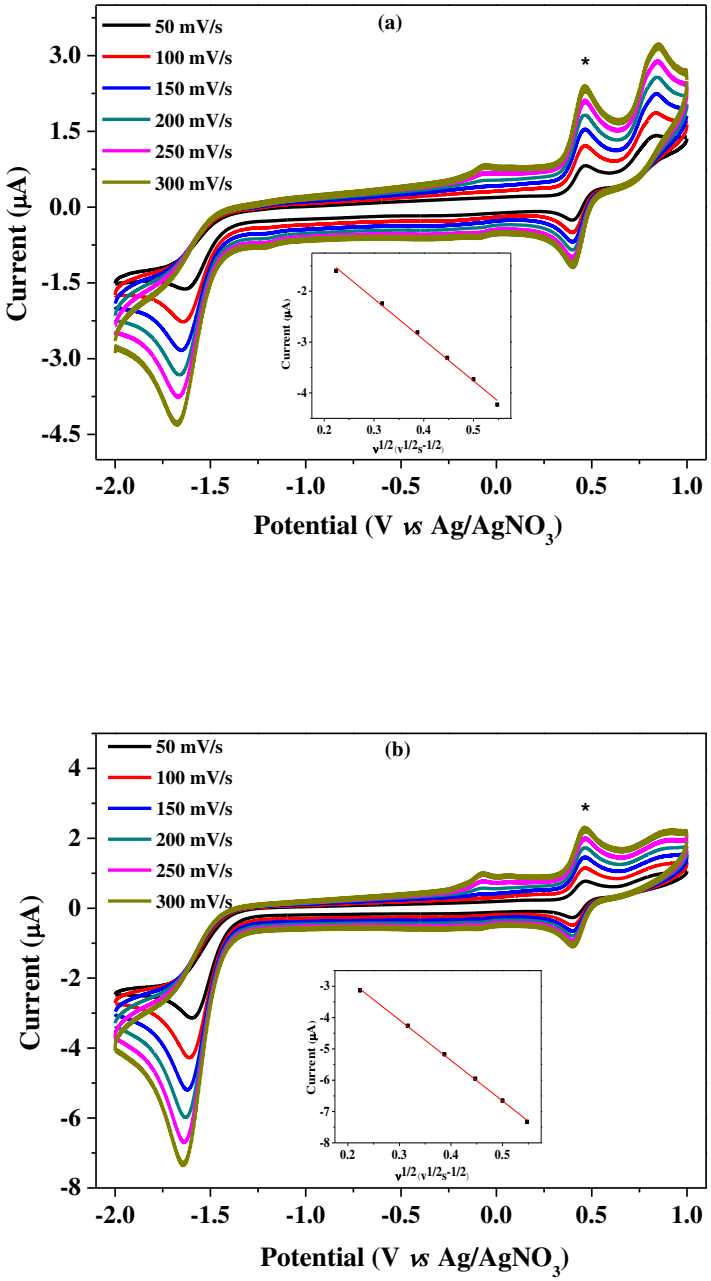

Fig. S7. (a) Scan rate dependence of precatalytic waves for a 0.76 mM solution of complex **1** with 0.10 M [n-Bu_4N]ClO_4, at scan rates from 50 to 300 mV/s. (b) Scan rate dependence of precatalytic waves for a 1.26 mM solution of $Pt(PPh_3)_2Cl_2$ with 0.10 M [n-Bu_4N]ClO_4, at scan rates from 50 to 300 mV/s.

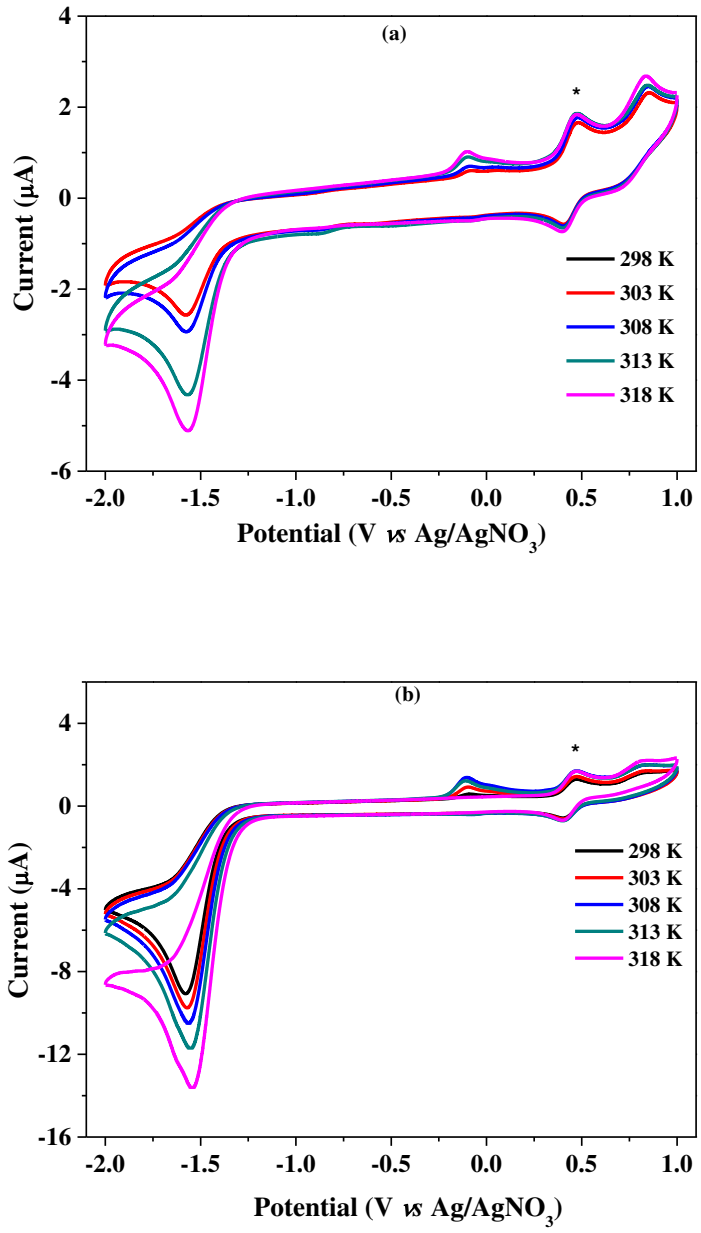

Fig. S8. Temperature dependence of cyclic voltammograms for a 0.10 M [n-Bu_4N]ClO_4 DMF solution with 3.40 mM of complex **1** (a), and 3.40 mM $Pt(PPh_3)_2Cl_2$.

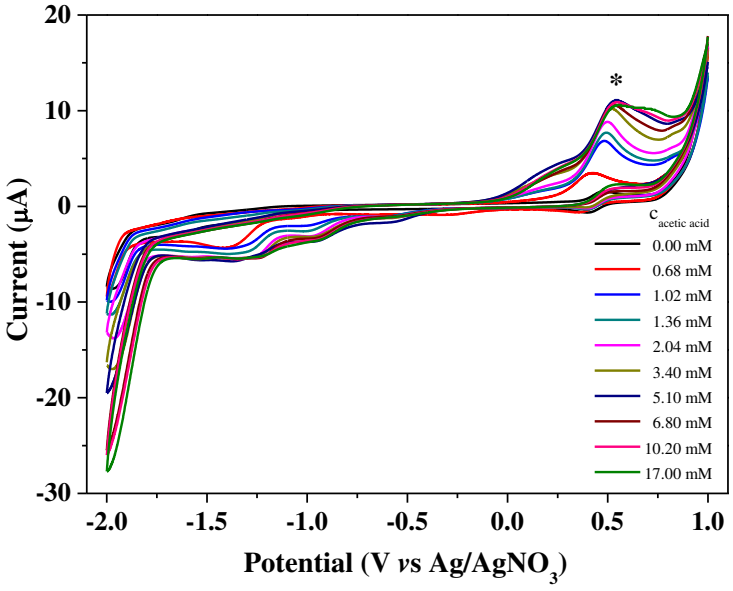

Fig. S9. CVs of 2.50 mM solution of HL with varying concentrations of acetic acid in DMF. Conditions: 0.10 M [n-Bu_4N]ClO_4 as supporting electrolyte, scan rate: 100 mV/s, glassy carbon working electrode (1 mm diameter), Pt counter electrode, $Ag/AgNO_3$ reference electrode. Ferrocene internal standard (*).

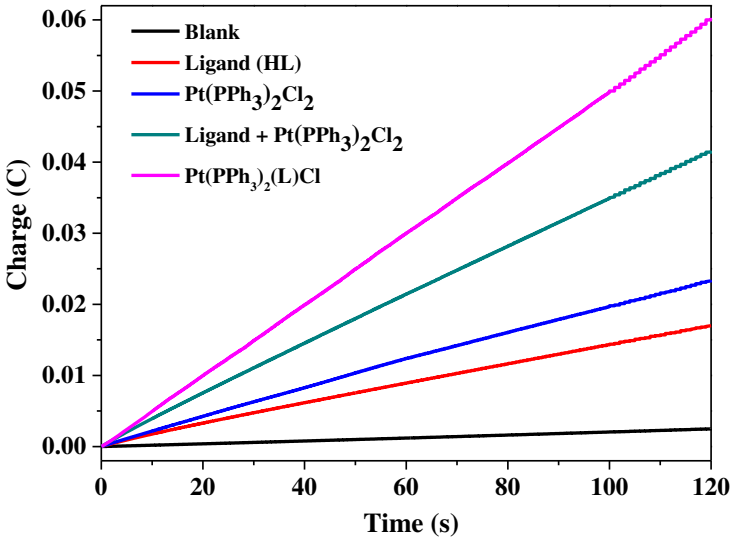

Fig. S10. Charge buildup versus time from electrolysis of blank (black), 9.32 μM HL (red), 9.32 μM $Pt(PPh_3)_2Cl_2$ (blue), the mixture of 9.32 μM HL and 9.32 μM

$Pt(PPh_3)_2Cl_2$ (green), and 9.32 μM $Pt(PPh_3)_2(L)Cl$ (violet) in DMF (0.10 M [n-Bu_4N]ClO_4) under -1.45 V versus $Ag/AgNO_3$.

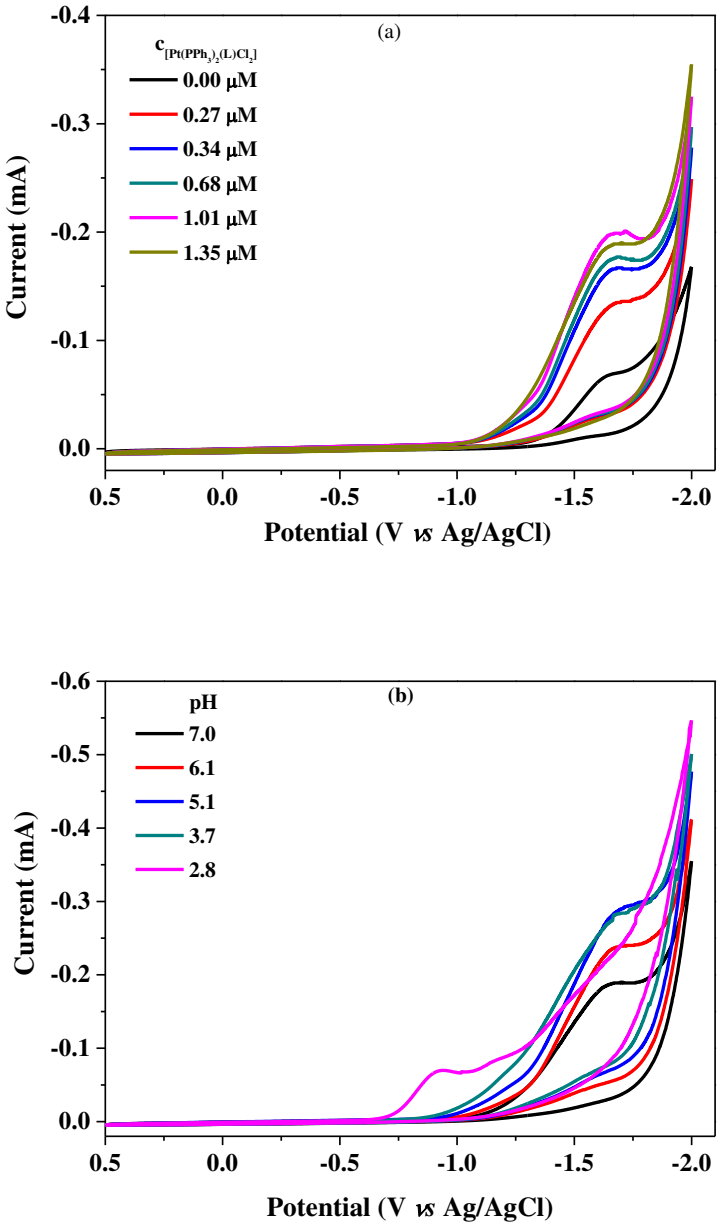

Fig. S11. (a) CVs of complex $Pt(PPh_3)_2Cl_2$ in different concentration. (b) CVs of $Pt(PPh_3)_2Cl_2$ (0.25 μM) in different pH. Conditions: Glassy carbon working electrode (1 mm diameter), Pt wire counter electrode, Ag/AgCl reference electrode.

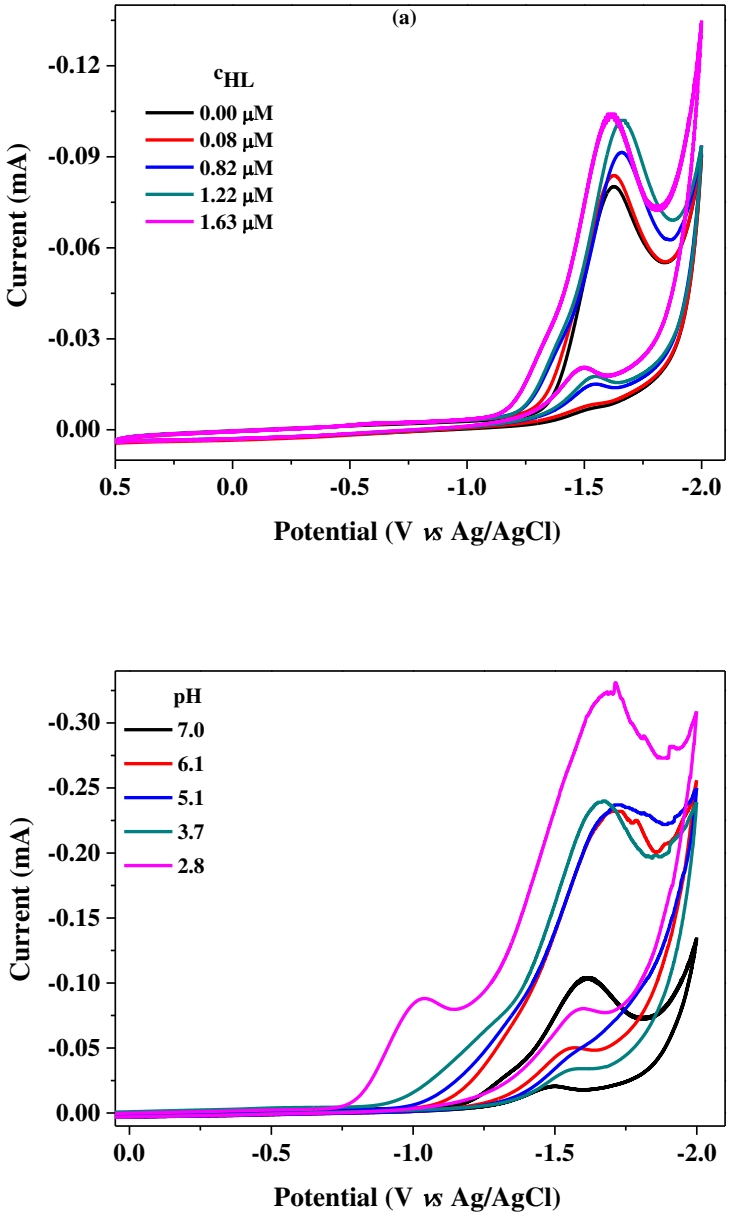

Fig. S12. (a) CVs of HL in different concentration. (b) CVs of HL (0.25 μM) in different pH. Conditions: 0.25 M phosphate buffered solution (pH 7.0), glassy carbon working electrode (1 mm diameter), Pt wire counter electrode, Ag/AgCl reference electrode.

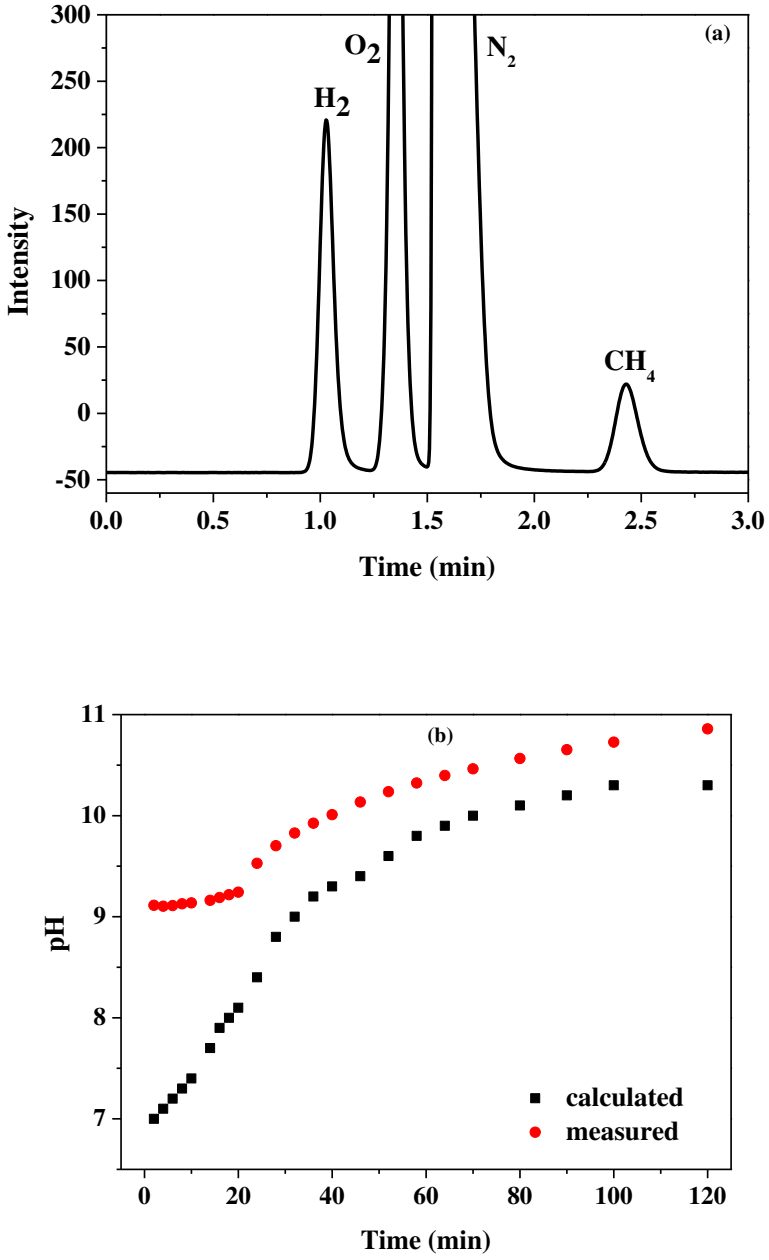

Fig. S13. (a) GC traces after a 1-h controlled-potential electrolysis at −1.45V *vs* Ag/AgCl of 2.33 μM $Pt(PPh_3)_2(L)Cl$ in 0.25 M phosphate buffer (pH 7.0). A standard of CH_4 was added for calibration purposes. (b) Measured (red) and calculated (black) pH changes assuming a 100% Faradic efficiency of complex during electrolysis. (the theoretical pH change over time can be calculated by the equation of $pH = 14 + \lg \frac{\sum It}{FV}$ where I = current (A), t = time (s), F = Faraday constant (96485 C/mol), V = solution volume (0.05 L).

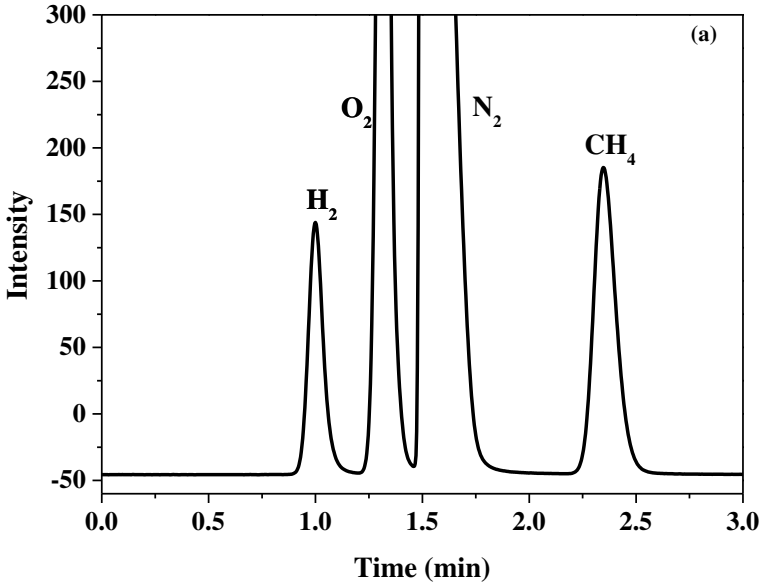

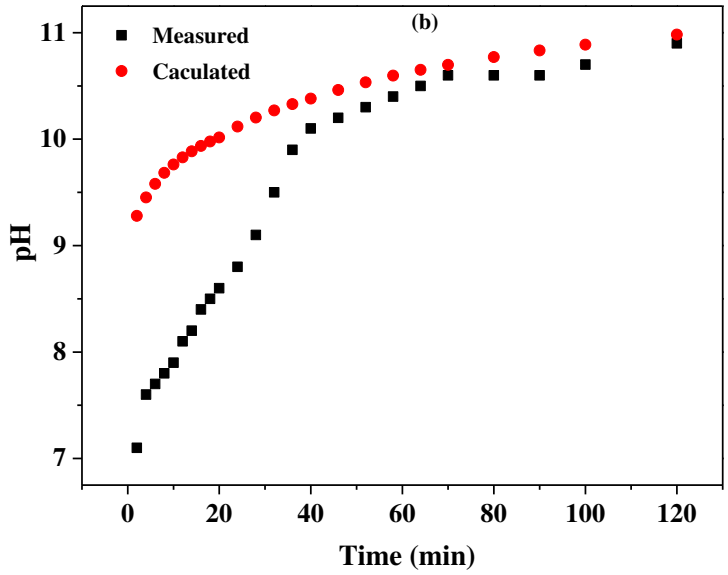

Fig. S14. (a) GC traces after a 1-h controlled-potential electrolysis at −1.45 V *vs* Ag/AgCl of 2.33 μM $Pt(PPh_3)_2Cl_2$ in 0.25 M phosphate buffer (pH 7.0). A standard of CH_4 was added for calibration purposes. (b) Measured (red) and calculated (black) pH changes assuming a 100% Faradic efficiency of complex during electrolysis. (the theoretical pH change over time can be calculated by the equation of

$pH = 14 + \lg \frac{\sum It}{FV}$ where I = current (A), t = time (s), F = Faraday constant (96485 C/mol), V = solution volume (0.05 L).

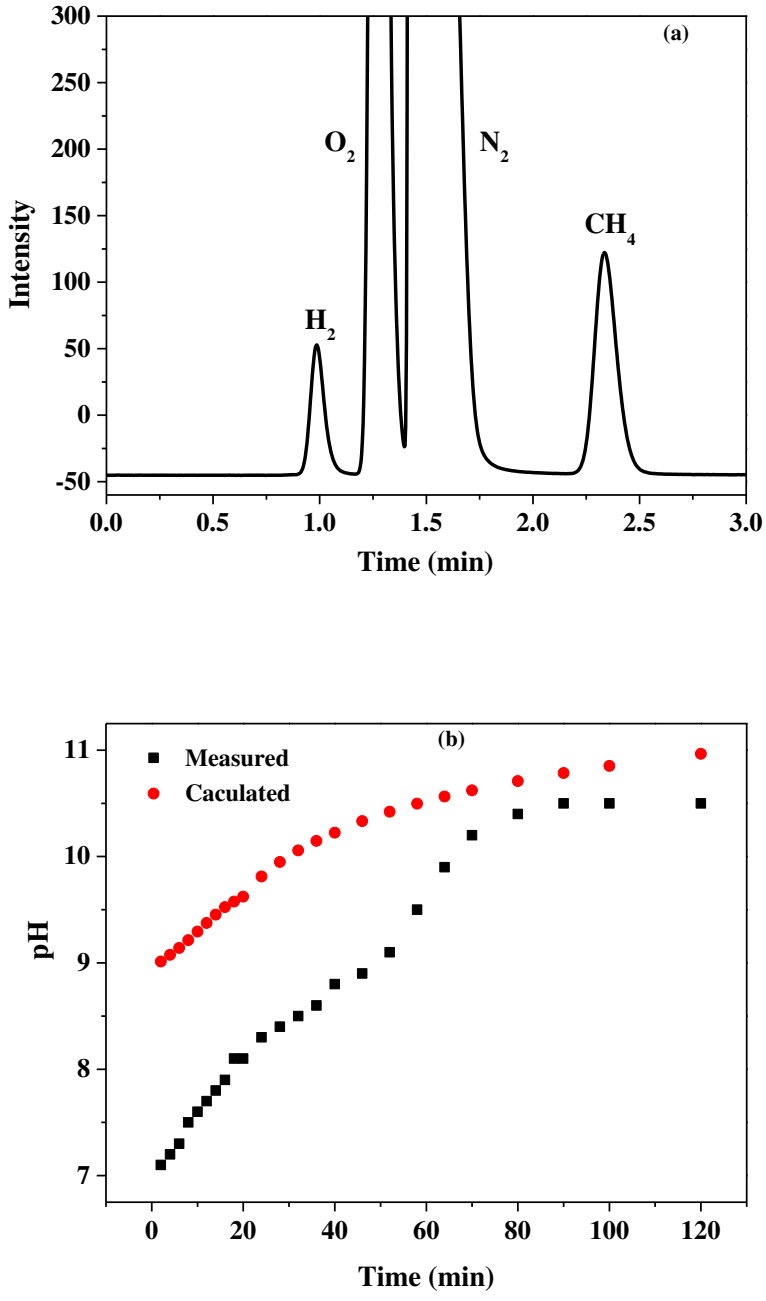

Fig. S15. (a) GC traces after a 1-h controlled-potential electrolysis at −1.45 V *vs* Ag/AgCl of 2.33 μM HL in 0.25 M phosphate buffer (pH 7.0). A standard of CH_4 was added for calibration purposes. (b) Measured (red) and calculated (black) pH changes assuming a 100% Faradic efficiency of complex during electrolysis. (the theoretical

pH change over time can be calculated by the equation of $pH = 14 + \lg \frac{\sum It}{FV}$ where I = current (A), t = time (s), F = Faraday constant (96485 C/mol), V = solution volume (0.05 L).

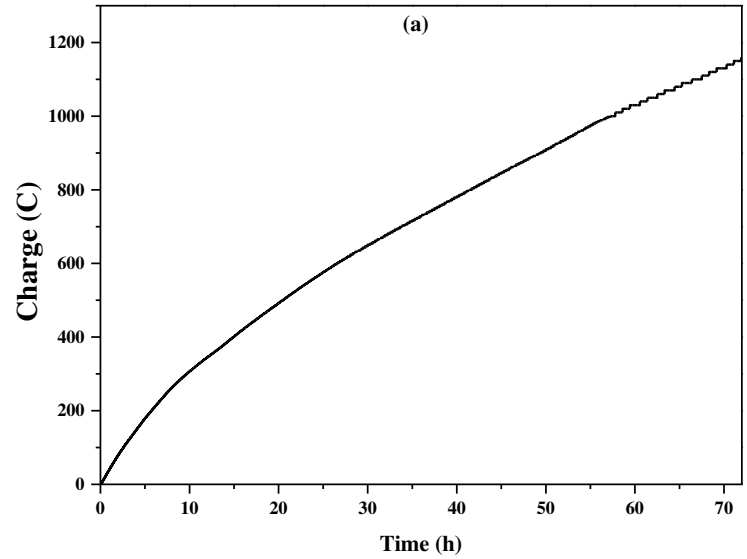

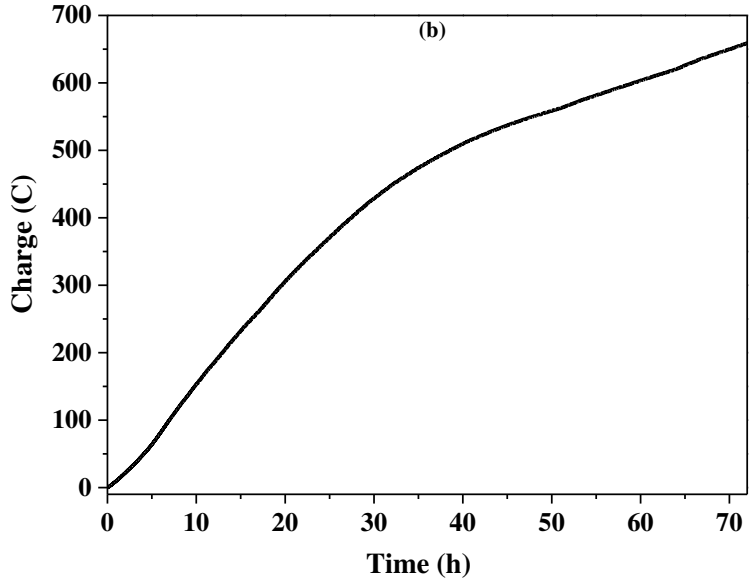

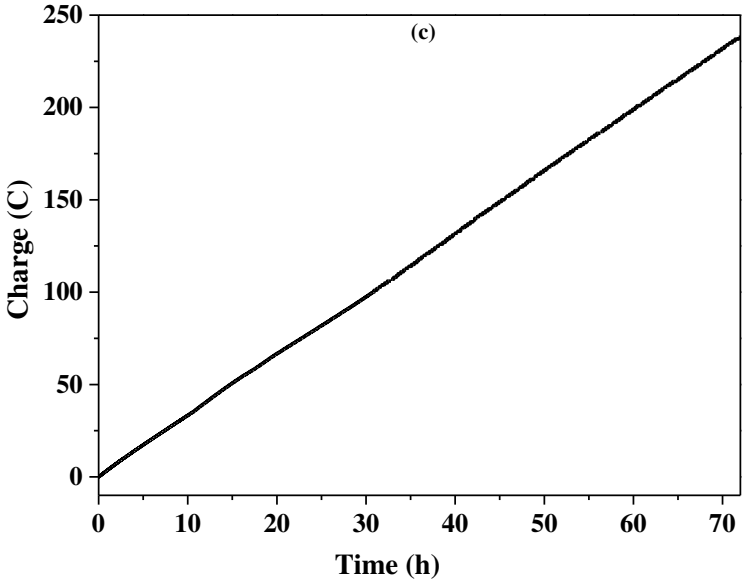

Fig. S16. (a) Charge buildup versus time from 2.33 μM complex **1** in a 0.25 M buffer (pH 7.0) under -1.45 V *vs* Ag/AgCl. (b) Charge buildup versus time from 2.33 μM $Pt(PPh_3)_2Cl_2$ in a 0.25 M buffer (pH 7.0) under -1.45 V *vs* Ag/AgCl. (c) Charge buildup versus time from 2.33 μM HL in a 0.25 M buffer (pH 7.0) under -1.45 V *vs* Ag/AgCl.

$$TOF = \frac{\Delta C}{F \cdot n_1 \cdot n_2 \cdot t} = \frac{0.0234C \times 3600}{96485C \cdot mol^{-1} \times 2 \times 0.373 \times 10^{-6} mol \times 120} = 9.84h^{-1}$$

Eq. S1. The calculation of TOF for $Pt(PPh_3)_2Cl_2$ (in DMF)

$$TOF = \frac{\Delta C}{F \cdot n_1 \cdot n_2 \cdot t} = \frac{0.0603C \times 3600}{96485C \cdot mol^{-1} \times 2 \times 0.373 \times 10^{-6} mol \times 120} = 25.36h^{-1}$$

Eq. S2. The calculation of TOF for $Pt(PPh_3)_2(L)Cl$ (in DMF)

$$TOF = \frac{\Delta C}{F \cdot n_1 \cdot n_2 \cdot t} = \frac{1.55C \times 3600}{96485C \cdot mol^{-1} \times 2 \times 0.373 \times 10^{-6} mol \times 120} = 651.87h^{-1}$$

Eq. S3. The calculation of TOF for $Pt(PPh_3)_2(L)Cl$ (in buffer, pH 7.0)

$$TOF = \frac{\Delta C}{F \cdot n_1 \cdot n_2 \cdot t} = \frac{0.583C \times 3600}{96485C \cdot mol^{-1} \times 2 \times 0.373 \times 10^{-6} mol \times 120} = 245.18h^{-1}$$

Eq. S4. The calculation of TOF for $(Pt(PPh_3)_2Cl_2$ (in buffer, pH 7.0).

$$TOF = \frac{\Delta C}{F \cdot n_1 \cdot n_2 \cdot t} = \frac{0.226C \times 3600}{96485C \cdot mol^{-1} \times 2 \times 0.373 \times 10^{-6} mol \times 120} = 95.06h^{-1}$$

Eq. S5. The calculation of TOF for HL (in buffer, pH 7.0)

Table S1. Crystallographic data for **HL** and $Pt(PPh_3)_2(L)Cl$ **1**

Parameter	HL	$Pt(PPh_3)_2(L)Cl$ **1**
Empirical formula	$C_{12}H_{12}N_4O$	$C_{52}H_{51}ClN_4O_3P_2Pt$
Formula weight	228.26	1072.45
λ (Å)	0.71073	0.71073
Crystal system	monoclinic	monoclinic
Space group	P2(1)/c	P2(1)/c
a/Å	18.961(4)	23.331(3)
b/Å	5.3302(11)	10.0888(13)
c/Å	25.673(10)	22.298(2)
α/°	90	90
β/°	115.89(2)	116.786(3)
γ/°	90	90
V/Å^3	2334.2(11)	4685.5(10)
Z	8	4
Dc/Mgm^{-3}	1.299	1.520
F(000)	960	2160
θ range for data collection	3.19 to 27.46°	3.28 to 27.48°
Reflections collected/unique	20901/5246	23259/10452
Data/restraints/parameters	5246/0/307	10452/0/538
Goodness-of-fit on F^2	0.940	1.070
Final R indices [I>2sigma(I)]	R1 = 0.0520	R1 = 0.0664
	wR2 = 0.1302	wR2 = 0.1664
R indices (all data)	R1 = 0.1278	R1 = 0.0828
	wR2 = 0.1817	wR2 = 0.1726

Table S2. Selected bond lengths (**Å**) and angles (o) for **HL** and $Pt(PPh_3)_2(L)Cl$ **1**

HL			
N(1)-N(2)	1.269(3)	N(1)-C(1)	1.422(3)
N(2)-N(3)	1.336(3)	N(3)-C(8)	1.388(3)
N(4)-C(8)	1.333(3)		
N(1)-N(2)-N(3)	110.6(2)	N(3)-C(8)-N(4)	113.6(2)
Complex 1			
Pt(1)-N(2)	2.038(7)	Pt(1)-P(1)	2.238(2)
Pt(1)-P(2)	2.270(2)	Pt(1)-Cl(1)	2.363(2)
N(3)-N(1)-N(2)	112.9(7)		